semiempirical absorption correction was applied.

Acknowledgment. R.R.S. thanks the National Institutes of Health for support through Grant GM-31978. The Biomedical Research Support Shared Instrumentation Grant Program, Division of Research Resources, provided funds for the purchase of the X-ray diffraction equipment (NIH Grant S10 RR02243). We thank Drs. W. M. Davis and S. Bott for help with the X-ray study.

Supplementary Material Available: A fully labeled drawing of W(DCP)$_4$Cl(Et$_2$O) and a table of final positional and thermal parameters (2 pages); a table of final observed and calculated structure factors (11 pages). Ordering information is given on any current masthead page.

Contribution from the Department of Chemistry, Faculty of Science, Tohoku University, Aoba, Aramaki, Sendai 980, Japan

A New Mixed Molybdenum-Tungsten Dinuclear Complex, Bis(μ-oxo)(μ-ethylenediaminetetraacetato-*N*,*N*')oxomolybdenum(V)oxotungstate(V)

Shinji Ikari, Yoichi Sasaki,* Akira Nagasawa, Chizuko Kabuto, and Tasuku Ito*

Received August 30, 1988

Neutralization by aqueous 2 M Na_2CO_3 of an aqueous solution of $(pyH)_2[MoOCl_5]$ (py = pyridine), $(NH_4)_2[WOCl_5]$, and disodium dihydrogen ethylenediaminetetraacetate (Na_2H_2edta) under a nitrogen atmosphere gave a mixture of $[Mo_2O_4(edta)]^{2-}$, $[W_2O_4(edta)]^{2-}$, and the new mixed-metal title complex. The new complex was purified by the use of an anion-exchange column (QAE-Sephadex A-25). The mixed-metal structure was confirmed by the XPS spectra, ^1H and ^{13}C NMR spectra, and the X-ray crystal structure determination. The sodium salt of the complex anion, $WMoNa_2O_{16.5}N_2C_{10}H_{21}$, crystallizes in the monoclinic space group $P2_1$ with a = 9.133 (1) Å, b = 32.119 (3) Å, c = 7.128 (1) Å, β = 101.97 (1)°, V = 2045.4 (4) Å^3, and Z = 4. The structure was solved by using 2691 unique reflections with $|F_o| > 3\sigma(F_o)$ to give R = 0.031. Two metal ions were statistically disordered. Each metal ion has a heavily distorted octahedral structure. The metal-metal distance is 2.55 (1) Å, indicating the existence of a direct metal-metal bond. $[MoWO_4(edta)]^{2-}$ exhibits an absorption peak at 288 nm (ϵ = 8200 M^{-1} cm^{-1}) and a distinctive shoulder at 352 nm (ϵ = 980 M^{-1} cm^{-1}). Both transitions are located between the corresponding peaks of the dimolybdenum(V) (298, 388 nm) and the ditungsten(V) (276, 342 nm) complexes. Cyclic voltammetry in an aqueous solution at pH 7.5 (phosphate buffer) shows one irreversible oxidation wave at +0.56 V vs SCE with a glassy-carbon electrode. ^{95}Mo and ^{183}W NMR signals appear at higher and lower field, respectively, than the corresponding signals of the two homonuclear dimers. The Mo 3d electron binding energies are smaller than those of the dimolybdenum(V) complex, while the W 4d and 4f electron binding energies are larger than those of the ditungsten(V) complex. Metal NMR and XPS data indicate that molybdenum and tungsten ions in the mixed-metal complex are in somewhat lower and higher oxidation states than those of the dimolybdenum and ditungsten complexes, respectively.

Introduction

Mixed-metal clusters without strong σ-donating and/or π-accepting ligands such as CO are important for investigating the nature of interactions between different metal atoms and regioselective redox and ligand substitution reactions. We have recently reported two types of new mixed-metal trinuclear complexes, $[Mo_nW_{3-n}(\mu_3\text{-}O)_2(\mu\text{-}CH_3COO)_6(H_2O)_3]^{2+}$ (n = 1, 2)[1] and $[Ru_2Rh(\mu_3\text{-}O)(\mu\text{-}CH_3COO)_6(L)_3]^+$ (L = H_2O, pyridine).[2] The important feature of these complexes is that their structural characteristics, such as bond lengths and angles, are very similar to those of their homonuclear analogues. It is thus possible in these cases to compare the electronic structures and the reactivities of the mixed-metal complexes with those of the homonuclear analogues without considering different steric factors. The X-ray photoelectron (XPS)[3] and metal (^{95}Mo and ^{183}W) NMR spectra[4] of the mixed Mo-W clusters revealed that a shifting of negative charge takes place from tungsten to molybdenum. This may result from the difference in electronegativities of the two metal atoms. It is interesting that the extent of the charge shift is large enough to be observed by the two techniques and yet the structural features are not significantly affected. A similar charge shift was not observed by XPS for the mixed Ru-Rh complex.[2] It was suggested that this may be because the metal-metal direct bond is essentially absent in this system (the Ru-Rh distance is expected to be ca. 3.3 Å,[2] while the Mo-W distances in the Mo-W clusters are ca. 2.73 Å[5]).[6] The rate of the substitution of methanol for the terminal water ligand is very similar between Ru and Rh sites in the Ru-Rh trinuclear complex.[2] In marked contrast, the Mo-W clusters show significant regioselectivity in their ligand substitution reactions (terminal water ligand substitution).[5] Obviously it is important to extend the research to other heterometallic systems to find more general examples.

Molybdenum and tungsten are unique in the sense that they give stable clusters in a wide range of oxidation states and that the structural characteristics of the corresponding clusters are very similar between the two elements.[7-10] In lower oxidation states (bivalent and tervalent), there have been a variety of mixed molybdenum-tungsten dinuclear complexes reported with metal-metal multiple bonds.[11-21] Trinuclear mixed Mo-W complexes,

(1) Wang, B.; Sasaki, Y.; Nagasawa, A.; Ito, T. *J. Am. Chem. Soc.* **1986**, *108*, 6059-6060.
(2) Sasaki, Y.; Tokiwa, A.; Ito, T. *J. Am. Chem. Soc.* **1987**, *109*, 6341-6347.
(3) Wang, B.; Sasaki, Y.; Ikari, S.; Kimura, K.; Ito, T. *Chem. Lett.* **1987**, 1955-1958.
(4) Nagasawa, A.; Sasaki, Y.; Wang, B.; Ikari, S.; Ito, T. *Chem. Lett.* **1987**, 1271-1274.
(5) Wang, B. Ph.D. Thesis, Tohoku University, 1988.
(6) Indirect interaction between metal atoms through the central oxygen atom is obvious from the absorption spectra. Thus, the failure to observe a charge shift might be due to the small difference in electronegativity between Ru and Rh rather than the absence of a Ru-Rh bond.
(7) Cotton, F. A.; Wilkinson, G. *Advanced Inorganic Chemistry*, 5th ed.; Wiley: New York, 1988; pp 804-847.
(8) Greenwood, N. N.; Earnshaw, A. *Chemistry of the Elements*; Pergamon Press: Elmsford, NY, 1984; p 1167.
(9) Stiefel, E. I. *Prog. Inorg. Chem.* **1977**, *22*, 1-223.
(10) Dori, Z. *Prog. Inorg. Chem.* **1981**, *28*, 239-307.
(11) Katovic, V.; Templeton, J. L.; Hoxmeier, R. J.; McCarley, R. E. *J. Am. Chem. Soc.* **1975**, *97*, 5300-5302.
(12) Katovic, V.; McCarley, R. E. *J. Am. Chem. Soc.* **1978**, *100*, 5586-5587.
(13) Katovic, V.; McCarley, R. E. *Inorg. Chem.* **1978**, *17*, 1268-1270.
(14) Cotton, F. A.; Hanson, B. E. *Inorg. Chem.* **1978**, *17*, 3237-3240.
(15) Bursten, B. E.; Cotton, F. A.; Cowley, A. H.; Hanson, B. E.; Lattman, M.; Stanley, G. G. *J. Am. Chem. Soc.* **1979**, *101*, 6244-6249.

0020-1669/89/1328-1248$01.50/0

in addition to the above example, have also been reported.[17,22] Although the evidence is indirect, charge polarization between Mo and W has been postulated in some of these cases.[11,17,19,23]

A mixed Mo–W cluster of quinquevalent metal ions has not yet been reported. Molybdenum(V)[9,24–29] and tungsten(V)[10,30–32] are known to give dimeric complexes with a $M_2(O)_2(\mu\text{-}O)_2$ core. Formally, a metal–metal single bond is assumed for these dinuclear complexes as in the above mentioned trinuclear complexes. The metal–metal distances are shorter (2.5–2.6 Å) than the corresponding ones in the trinuclear complexes of molybdenum(IV) and tungsten(IV), and stronger metal–metal interactions may be expected. In this paper, we report a new mixed molybdenum–tungsten complex with this dinuclear core. The ethylenediaminetetraacetate ligand was chosen since this ligand gave the most stable compounds with the M_2O_4 core[31,33–39] and was appropriate for the time-consuming purification procedure. With the present new complex, a series of mixed Mo–W cluster complexes from divalent to quinquevalent states is now completed. The comparison of the data for the new complex with those of the trinuclear complexes should reveal the influence of the oxidation state, metal–metal bond distance, and number of neighboring metal ions. The X-ray photoelectron spectrum of the new complex has been reported in our preliminary account.[3]

Experimental Section

Preparations of the Complexes. (1) $Na_2[MoW(O)_2(\mu\text{-}O)_2(\mu\text{-edta})]\cdot 4.5H_2O$. To a chilled aqueous solution (50 cm³) of $Na_2H_2edta\cdot 2H_2O$ (11 g, 0.030 mol) were added $(pyH)_2[Mo^VOCl_5]$[40] (py = pyridine) (8 g, 0.018 mol) and $(NH_4)_2[W^VOCl_5]$[41] (5 g, 0.012 mol) under a nitrogen atmosphere, and the solution was neutralized slowly with aqueous 2 M Na_2CO_3 solution and filtered. The filtrate was diluted with water (ca. 10 dm³) and treated with three successive anion-exchange columns of QAE-Sephadex A-25 in the Cl^- form (3 cm in diameter and 80 cm in length). Elution of the brown band with 0.12 M $NaClO_4$ (3 dm³ per day) allowed the separation and isolation of three components after 1 month. These turned out to be $[W_2(O)_2(\mu\text{-}O)_2(\mu\text{-edta})]^{2-}$, $[MoW(O)_2(\mu\text{-}O)_2(\mu\text{-edta})]^{2-}$, and $[Mo_2(O)_2(\mu\text{-}O)_2(\mu\text{-edta})]^{2-}$ in elution order. The eluate of the mixed-metal complex anion was evaporated to ca. 50 cm³, and the resulting sodium perchlorate was removed by filtration. Finally, ethanol was added until the filtrate just turned cloudy. When it was cooled in a refrigerator, orange crystals of $Na_2[MoW(O)_2(\mu\text{-}O)_2(\mu\text{-edta})]\cdot 4.5H_2O$ were obtained; yield ca. 0.3 g (4% based on $(NH_4)_2[WOCl_5]$). Anal. Calcd for $C_{10}H_{21}N_2O_{16.5}Na_2MoW$: C, 15.82; H, 2.79; N, 3.69. Found: C, 16.01; H, 2.86; N, 4.08. When the crystals were dried in vacuo, they effloresced by losing their crystalline waters. Anal. Calcd for $C_{10}H_{12}N_2O_{12}Na_2MoW$ (anhydrous salt): C, 17.72; H, 1.78; N, 4.13. Found: C, 17.88; H, 2.38; N, 4.18. IR (cm^{-1}): 3440 w, 1639 s, 1447 w, 1398 m, 1380 m, 1357 m, 1238 w, 942 s, 910 m, 870 m, 760 m, 718 w, 651 w, 588 w, 513 m, 485 m, 463 w, 416 w. For most measurements, the air-stable anhydrous salt was used.

(2) Other Complexes. The known complexes $Na_2[Mo_2(O)_2(\mu\text{-}O)_2(\mu\text{-edta})]$[33] and $Na_2[W_2(O)_2(\mu\text{-}O)_2(\mu\text{-edta})]\cdot 3H_2O$[38] were obtained from the corresponding eluates obtained during the preparation of $Na_2[MoW(O)_2(\mu\text{-}O)_2(\mu\text{-edta})]\cdot 4.5H_2O$. $Na_2[Mo_2(O)_2(\mu\text{-}O)_2(\mu\text{-edta})]$ was also prepared from $[Mo_2(O)_2(\mu\text{-}O)_2(C_2O_4)_2(H_2O)_2]^{2-}$[42] and purified by the use of a QAE-Sephadex A-25 anion-exchange column. $Na_2[W_2(O)_2(\mu\text{-}O)_2(\mu\text{-edta})]\cdot 3H_2O$ was prepared by modifying the literature method.[38] The ammonium salt of the oxalato complex of tungsten(V)[41] (7.1 g) was added to an aqueous solution (175 cm³) containing H_4edta (6.3 g) and anhydrous sodium acetate (7.0 g). The solution was mixed with an aqueous solution (150 cm³) of $CaCl_2\cdot 2H_2O$ (5.4 g). The precipitate (CaC_2O_4) was filtered off, and $BaCl_2\cdot 2H_2O$ (18.6 g) in 150 cm³ of water was added to the filtrate. A brown precipitate was removed by filtration. The filtrate was diluted with a large amount of water (10 dm³) and poured onto the column of QAE-Sephadex A-25 resin. The column was washed with water. The brown band was eluted with 0.15 M $NaClO_4$. The eluate was concentrated to ca. 50 cm³, and $NaClO_4$ was removed. On addition of ethanol to the concentrate, orange crystals of $Na_2[W_2(O)_2(\mu\text{-}O)_2(\mu\text{-edta})]\cdot 3H_2O$ were obtained; yield 4.0 g (50%).

Other Materials. Anhydrous sodium perchlorate, $Na_2H_2edta\cdot 2H_2O$, and H_4edta were used as received.

Measurements. Ultraviolet and visible absorption spectra were measured by using a Hitachi 330 and 340 spectrophotometers. Infrared absorption spectra were measured on a Jasco IR 810 spectrophotometer

Table I. Crystallographic Data for $Na_2[MoW(O)_2(\mu\text{-}O)_2(\mu\text{-edta})]\cdot 4.5H_2O$

$WMoNa_2O_{16.5}N_2C_{10}H_{21}$	fw = 759.05
a = 9.133 (1) Å	space group $P2_1$ (No. 4)
b = 32.119 (3) Å	T = 13 °C
c = 7.128 (1) Å	λ = 0.710 69 Å
β = 101.97 (1)°	ρ_{obsd} = 2.43 g cm^{-3}, ρ_{calcd} = 2.47 g cm^{-3}
V = 2045.4 (4) Å^3	μ = 66.94 cm^{-1}
Z = 4	$R(F_o)$ = 0.0310
	$R_w(F_o^2)$ = 0.0348

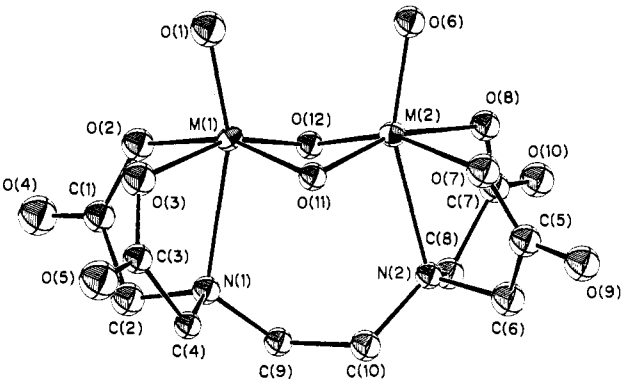

Figure 1. Structure of one of the two crystallographically independent $[MoW(O)_2(\mu\text{-}O)_2(\mu\text{-edta})]^{2-}$ ions (molecule A) and atomic numbering scheme. The thermal ellipsoids are drawn at the 50% probability level.

(16) Luck, R. L.; Morris, R. H. *J. Am. Chem. Soc.* **1984**, *106*, 7978–7979.
(17) Chisholm, M. H.; Folting, K.; Huffman, J. C.; Kober, E. M. *Inorg. Chem.* **1985**, *24*, 241–245.
(18) Bancroft, G. M.; Bice, J.-A.; Morris, R. H.; Luck, R. L. *J. Chem. Soc., Chem. Commun.* **1986**, 898–899.
(19) Luck, R. L.; Morris, R. H.; Sawyer, J. F. *Inorg. Chem.* **1987**, *26*, 2422–2429.
(20) Morris, R. H. *Polyhedron* **1987**, *6*, 793–801.
(21) Cotton, F. A.; Walton, R. A. *Multiple Bonds between Metal Atoms*; Wiley: New York, 1982.
(22) Chisholm, M. H.; Folting, K.; Heppert, J. A.; Hoffman, D. M.; Huffman, J. C. *J. Am. Chem. Soc.* **1985**, *107*, 1234–1241.
(23) Wang, B.; Sasaki, Y.; Nagasawa, A.; Ito, T. *J. Coord. Chem.* **1988**, *18*, 45–61.
(24) Mattes, R.; Lux, G. *Z. Anorg. Allg. Chem.* **1976**, *424*, 173–182.
(25) Jezowska-Trzebiatowska, B.; Glowiak, T.; Rudolf, M. F.; Sabat, M.; Sabat, T. *Russ. J. Inorg. Chem. (Engl. Transl.)* **1977**, *22*, 1590–1597.
(26) Kojima, A.; Ooi, S.; Sasaki, Y.; Suzuki, K. Z.; Saito, K.; Kuroya, H. *Bull. Chem. Soc. Jpn.* **1981**, *54*, 2457–2465.
(27) Shibahara, T.; Kuroya, H.; Matsumoto, K.; Ooi, S. *Inorg. Chim. Acta* **1981**, *54*, L75–L76.
(28) Cotton, F. A.; Ilsley, W. H. *Inorg. Chim. Acta* **1982**, *59*, 213–217.
(29) Dahlstrom, P. L.; Hyde, J. R.; Vella, P. A.; Zubieta, J. *Inorg. Chem.* **1982**, *21*, 927–932.
(30) Mattes, R.; Mennemann, K. *Z. Anorg. Allg. Chem.* **1977**, *437*, 175–182.
(31) (a) Khalil, S.; Sheldrick, B.; Soares, A. B.; Sykes, A. G. *Inorg. Chim. Acta* **1977**, *25*, L83–L84. (b) Khalil, S.; Sheldrick, B. *Acta Crystallogr., Sect. B: Struct. Crystallogr. Cryst. Chem.* **1978**, *B34*, 3751–3753.
(32) Schreiber, P.; Wieghardt, K.; Florke, U.; Haupt, H.-J. *Inorg. Chem.* **1988**, *27*, 2111–2115.
(33) Pecsok, R. L.; Sawyer, D. T. *J. Am. Chem. Soc.* **1956**, *78*, 5495–5500.
(34) Haynes, L. V.; Sawyer, D. T. *Inorg. Chem.* **1967**, *6*, 2146–2150.
(35) Sasaki, Y.; Sykes, A. G. *J. Chem. Soc., Dalton Trans.* **1974**, 1468–1473.
(36) Blackmer, G. L.; Johnson, K. J.; Roberts, R. L. *Inorg. Chem.* **1976**, *15*, 596–601.
(37) Ott, V. R.; Swieter, D. S.; Schultz, F. A. *Inorg. Chem.* **1977**, *16*, 2538–2545.
(38) Novak, J.; Podlaha, J. *J. Inorg. Nucl. Chem.* **1974**, *36*, 1061–1065.
(39) Soares, A. B.; Taylor, R. C.; Sykes, A. G. *J. Chem. Soc., Dalton Trans.* **1980**, 1101–1104.
(40) Sasaki, Y.; Taylor, R. S.; Sykes, A. G. *J. Chem. Soc., Dalton Trans.* **1975**, 396–400.
(41) Collenberg, O. *Z. Anorg. Chem.* **1918**, *102*, 247–276.
(42) Cotton, F. A.; Morehouse, S. M. *Inorg. Chem.* **1965**, *4*, 1377–1381.

Table II. Atomic Positional Parameters of $Na_2[MoW(O)_2(\mu\text{-}O)_2(\mu\text{-edta})]\cdot 4.5H_2O$[a]

atom	x	y	z	B_{iso}, Å^2	atom	x	y	z	B_{iso}, Å^2
M(A1)	8359 (8)	393 (3)	11089 (10)	1.3[b]	O(B6)	1014 (12)	1948 (3)	5602 (15)	2.2 (2)
M(A2)	-18903 (8)	0	-6485 (10)	1.3[b]	O(B7)	2733 (13)	2647 (3)	5663 (15)	2.6 (2)
O(A1)	658 (11)	339 (3)	3123 (14)	2.0 (2)	O(B8)	3217 (12)	1860 (3)	3530 (14)	2.0 (2)
O(A2)	2648 (11)	444 (3)	837 (14)	1.8 (2)	O(B9)	4210 (16)	3190 (5)	6226 (20)	4.5 (3)
O(A3)	2272 (12)	-383 (3)	2703 (15)	2.2 (2)	O(B10)	4601 (13)	1598 (3)	1605 (15)	2.5 (2)
O(A4)	4062 (12)	716 (3)	-1017 (15)	2.3 (2)	O(B11)	457 (11)	2007 (3)	1340 (14)	1.7 (2)
O(A5)	4171 (12)	-818 (3)	2952 (15)	2.5 (2)	O(B12)	80 (11)	2721 (3)	3415 (13)	1.6 (2)
O(A6)	-2703 (12)	296 (3)	888 (15)	2.5 (2)	N(B1)	-747 (13)	2766 (4)	-787 (15)	1.3 (2)
O(A7)	-3150 (12)	324 (3)	-3011 (14)	2.0 (2)	N(B2)	2876 (14)	2605 (4)	1902 (16)	1.6 (2)
O(A8)	-3503 (12)	-449 (3)	-1045 (15)	2.3 (2)	C(B1)	-2622 (18)	3157 (5)	423 (22)	2.1 (3)
O(A9)	-4352 (13)	340 (4)	-6011 (16)	3.0 (2)	C(B2)	-1209 (17)	3188 (5)	-342 (20)	1.8 (3)
O(A10)	-4042 (13)	-1122 (4)	-1632 (17)	3.0 (2)	C(B3)	-2796 (16)	2279 (5)	-2345 (19)	1.9 (3)
O(A11)	-571 (11)	-401 (3)	762 (13)	1.5 (2)	C(B4)	-1724 (18)	2625 (5)	-2622 (22)	2.2 (3)
O(A12)	-261 (10)	338 (3)	-1185 (13)	1.5 (2)	C(B5)	3642 (19)	2906 (5)	5164 (23)	2.5 (3)
N(A1)	2103 (13)	-249 (4)	-1125 (16)	1.4 (2)	C(B6)	4120 (17)	2820 (5)	3274 (21)	1.9 (3)
N(A2)	-1638 (13)	-402 (4)	-3387 (16)	1.6 (2)	C(B7)	3858 (17)	1887 (5)	2065 (20)	1.6 (3)
C(A1)	3193 (17)	446 (5)	-680 (21)	1.8 (3)	C(B8)	3581 (15)	2278 (5)	871 (18)	1.5 (2)
C(A2)	2691 (16)	99 (5)	-2140 (20)	1.9 (3)	C(B9)	834 (17)	2778 (5)	-1128 (20)	1.9 (3)
C(A3)	3270 (18)	-571 (5)	2022 (21)	2.0 (3)	C(B10)	2082 (18)	2924 (5)	492 (21)	2.0 (3)
C(A4)	3407 (18)	-480 (5)	-26 (22)	2.3 (3)	Na(1)	55513 (67)	9723 (19)	-32248 (82)	2.1[b]
C(A5)	-3456 (17)	165 (5)	-4716 (21)	1.9 (3)	Na(2)	59454 (72)	9092 (21)	18084 (86)	2.5[b]
C(A6)	-2777 (18)	-243 (5)	-5076 (22)	2.2 (3)	Na(3)	-56379 (65)	37017 (19)	-15678 (83)	2.1[b]
C(A7)	-3297 (17)	-870 (5)	-1808 (20)	1.8 (3)	Na(4)	20014 (76)	13088 (21)	-30844 (101)	2.9[b]
C(A8)	-2061 (16)	-832 (4)	-2914 (19)	1.5 (2)	Ow(1)	4394 (12)	1598 (3)	-2353 (15)	2.4 (2)
C(A9)	1239 (17)	-558 (5)	-2512 (21)	1.8 (3)	Ow(2)	7458 (13)	1193 (4)	-345 (16)	2.7 (2)
C(A10)	-117 (16)	-397 (5)	-3966 (20)	1.6 (2)	Ow(3)	89 (12)	5882 (3)	4197 (15)	2.3 (2)
M(B1)	-12520 (9)	23128 (3)	17590 (11)	1.5[b]	Ow(4)	-8197 (13)	3867 (4)	-2287 (16)	2.9 (2)
M(B2)	13924 (8)	22328 (3)	37846 (10)	1.2[b]	Ow(5)	9093 (14)	6271 (4)	293 (18)	3.4 (2)
O(B1)	-2219 (13)	2059 (3)	3165 (15)	2.5 (2)	Ow(6)	145 (14)	-1481 (4)	-4712 (17)	3.0 (2)
O(B2)	-2842 (11)	2808 (3)	1254 (14)	2.0 (2)	Ow(7)	3199 (13)	1011 (4)	-5558 (16)	2.9 (2)
O(B3)	-2463 (12)	2069 (3)	-761 (14)	2.1 (2)	Ow(8)	7101 (13)	1255 (4)	-5309 (15)	2.6 (2)
O(B4)	-3474 (13)	3453 (4)	358 (16)	2.8 (2)	Ow(9)	-6936 (16)	-1338 (4)	-4491 (20)	4.5 (3)
O(B5)	-3881 (12)	2207 (4)	-3605 (14)	2.5 (2)					

[a] Atomic numbering of the complex anion is shown in Figure 1. Metal and sodium atom positional parameters have been multiplied by 10^5 and other positional parameters by 10^4. [b] $B_{eq} = {}^3/_4\sum_i\sum_j\beta_{ij}\mathbf{a}_i\cdot\mathbf{a}_j$.

with KBr pellets at room temperature. ^{1}H NMR spectra (270 MHz) were measured on a JEOL GSX-270 FT-NMR spectrometer at 80 °C. ^{13}C NMR spectra (50.2 MHz) were obtained by a Varian XL-200 FT-NMR spectrometer at 28 ± 1 °C. ^{95}Mo and ^{183}W NMR spectra (32.59 and 20.84 MHz, respectively) were measured on a JEOL JNM-GX-500 FT-NMR spectrometer at 20–24 °C. X-ray photoelectron spectra were obtained by a VG-ESCA LAB Mark II instrument using Mg Kα exciting radiation at ambient temperature and pressures less than 10^{-9} Torr. The energy scale was calibrated by emission from the C 1s (methylene carbon) line at 284.6 eV. Samples were prepared as thin films on Al foil stuck to a Ni metal plate by evaporating acetonitrile solutions. When the peak intensities were compared among the three edta complexes (hereafter abbreviated as Mo_2, MoW, and W_2), the intensity was normalized with reference to Na 1s or C 1s peak intensities. Electrochemical measurements were carried out by using a Yanaco P-1100 polarographic analyzer with glassy carbon as the working electrode at 24 ± 2 °C. Potentials were recorded vs SCE.

Crystal Structure Determination. Crystals of $Na_2[MoW(O)_2(\mu\text{-}O)_2(\mu\text{-edta})]\cdot 4.5H_2O$ were obtained by slow crystallization (over 1 month) from the water–ethanol solution. A crystal with dimensions 0.2 × 0.2 × 0.25 mm was attached to a glass fiber and mounted on a Rigaku AFC-5R four-circle diffractometer equipped with a rotating anode (40 kV, 200 mA). The unit cell parameters were obtained by a least-squares refinement of the angular settings of 25 high-angle ($2\theta \approx 30°$) reflections. Crystallographic data are listed in Table I.[43] Data collection parameters are given as supplementary material. Intensity data were corrected for Lorentz and polarization factors. No absorption correction was made.

The structure was solved by heavy-atom methods and refined by the block-diagonal least-squares method. From the systematic extinction ($k = 2n$), the space group was either $P2_1/m$ or $P2_1$. The space group $P2_1/m$ was ruled out, since the structure was successfully solved to be $P2_1$. There are two crystallographically independent complexes in the asymmetric unit. Positions of molybdenum and tungsten atoms were found to be disordered. Accordingly, a mean scattering factor of (Mo + W)/2 was used for each metal atom. Thereupon, the refinement converged smoothly. The final refinement with anisotropic thermal parameters for the metal atoms, including Na, gave $R = 0.031$.[44] Hydrogen atoms were not included in the analysis.

Table III. Selected Interatomic Distances (Å) for $[MoW(O)_2(\mu\text{-}O)_2(\mu\text{-edta})]^{2-}$

	molecule A	molecule B
M(1)–M(2)	2.548 (1)	2.557 (1)
M(1)–O(1)	1.76 (1)	1.68 (1)
M(1)–O(2)	2.14 (1)	2.13 (1)
M(1)–O(3)	2.06 (1)	2.06 (1)
M(1)–O(11)	1.89 (1)	1.92 (1)
M(1)–O(12)	1.979 (9)	1.998 (9)
M(1)–N(1)	2.34 (1)	2.44 (1)
M(2)–O(6)	1.73 (1)	1.68 (1)
M(2)–O(7)	2.11 (1)	2.09 (1)
M(2)–O(8)	2.04 (1)	2.09 (1)
M(2)–O(11)	1.903 (9)	1.918 (9)
M(2)–O(12)	1.94 (1)	1.96 (1)
M(2)–N(2)	2.39 (1)	2.41 (1)

All calculations were performed with the Universal Crystallographic Computer Program System UNICS III[45] on an ACOS-1000 computer at the Computer Center of Tohoku University.

Atomic positional parameters are given in Table II. Tables of the structure factors and thermal parameters and a stereoscopic view of the unit cell of $Na_2[MoW(O)_2(\mu\text{-}O)_2(\mu\text{-edta})]\cdot 4.5H_2O$ are available as supplementary material.

Results

Description of the Structure. There are two crystallographically independent complex anions in the asymmetric unit of Na_2-

(43) As there was a possibility of overlapping of reflections with high 2θ values ($b = 32.119$ (2) Å) in the data collection with use of Mo Kα radiation, the measurements were carried out by using the ω scan mode. Each reflection peak was sharp enough to take the scan width to be $0.8 + 0.35 \tan\theta$. Although small overlaps were actually observed for some strong and high-angle reflections, we believe that this had no serious effect on the results of the present analysis.

(44) Least-squares refinement with anisotropic thermal parameters for all the non-hydrogen atoms was unsuccessful, because the number of observed intensity data was insufficient as compared with the number of parameters.

(45) Sakurai, T.; Kobayashi, K. *Rikagaku Kenkyusho Hokoku* **1979**, *55*, 69–77.

Table IV. Selected Interatomic Angles (deg) for $[MoW(O)_2(\mu\text{-}O)_2(\mu\text{-edta})]^{2-}$

	molecule A	molecule B
M(2)–M(1)–O(1)	100.5 (3)	99.6 (4)
M(2)–M(1)–O(2)	132.8 (3)	134.5 (3)
M(2)–M(1)–O(3)	133.2 (3)	136.7 (3)
M(2)–M(1)–O(11)	48.0 (3)	48.2 (3)
M(2)–M(1)–O(12)	48.9 (3)	49.0 (3)
M(2)–M(1)–N(1)	102.5 (3)	100.2 (3)
O(1)–M(1)–O(2)	86.9 (4)	92.2 (5)
O(1)–M(1)–O(3)	93.8 (4)	94.8 (5)
O(1)–M(1)–O(11)	109.9 (5)	112.9 (5)
O(1)–M(1)–O(12)	107.0 (4)	107.3 (5)
O(1)–M(1)–N(1)	155.5 (4)	159.5 (4)
O(2)–M(1)–O(3)	92.0 (4)	85.0 (4)
O(2)–M(1)–O(11)	163.1 (4)	154.5 (4)
O(2)–M(1)–O(12)	84.2 (4)	85.5 (4)
O(2)–M(1)–N(1)	71.3 (4)	70.0 (4)
O(3)–M(1)–O(11)	85.2 (4)	88.6 (4)
O(3)–M(1)–O(12)	158.6 (4)	156.3 (4)
O(3)–M(1)–N(1)	76.5 (4)	74.2 (4)
O(11)–M(1)–O(12)	92.3 (4)	90.8 (4)
O(11)–M(1)–N(1)	91.9 (4)	84.5 (4)
O(12)–M(1)–N(1)	82.3 (4)	82.1 (4)
M(1)–M(2)–O(6)	99.5 (3)	99.7 (4)
M(1)–M(2)–O(7)	133.2 (3)	131.0 (3)
M(1)–M(2)–O(8)	135.1 (3)	133.3 (3)
M(1)–M(2)–O(11)	47.7 (3)	48.3 (3)
M(1)–M(2)–O(12)	50.1 (3)	50.4 (3)
M(1)–M(2)–N(2)	100.3 (3)	102.1 (3)
O(6)–M(2)–O(7)	90.0 (5)	92.3 (5)
O(6)–M(2)–O(8)	94.8 (5)	92.9 (5)
O(6)–M(2)–O(11)	110.2 (5)	111.7 (5)
O(6)–M(2)–O(12)	105.3 (5)	108.8 (5)
O(6)–M(2)–N(2)	160.1 (4)	158.2 (4)
O(7)–M(2)–O(8)	88.8 (4)	92.8 (4)
O(7)–M(2)–O(11)	159.7 (4)	156.0 (5)
O(7)–M(2)–O(12)	83.2 (4)	80.7 (4)
O(7)–M(2)–N(2)	75.1 (4)	73.7 (4)
O(8)–M(2)–O(11)	87.4 (4)	85.2 (4)
O(8)–M(2)–O(12)	158.2 (4)	157.5 (4)
O(8)–M(2)–N(2)	72.2 (4)	71.7 (4)
O(11)–M(2)–O(12)	93.2 (4)	92.1 (4)
O(11)–M(2)–N(2)	84.7 (4)	83.0 (4)
O(12)–M(2)–N(2)	86.2 (4)	85.8 (4)
M(1)–O(11)–M(2)	84.3 (4)	83.6 (4)
M(1)–O(12)–M(2)	81.0 (4)	80.5 (4)

$[MoW(O)_2(\mu\text{-}O)_2(\mu\text{-edta})]\cdot 4.5H_2O$. The two complex ions have essentially the same structure.[46] An ORTEP drawing of one of the complex anions is shown in Figure 1 along with the atomic numbering scheme. Selected bond distances and angles are shown in Tables III and IV. Complete data tables are given as supplementary material. Each metal ion has a heavily distorted octahedral geometry. Although the two metal ions within a complex were not identified due to the disorder, the metal–metal bond distance is sufficiently short to assume a direct metal–metal bonding interaction.

Table V compares important bond distances and angles of the mixed-metal complex anion with those of the homonuclear complexes $[W_2(O)_2(\mu\text{-}O)_2(\mu\text{-edta})]^{2-}$[31] and $[Mo_2(O)_2(\mu\text{-}O)_2(\mu\text{-}R\text{-pdta})]^{2-}$ (*R*-pdta^{4-} = (*R*)-propylenediamine-*N*,*N*,*N*′,*N*′-tetraacetate(4−)).[26] The structure of $[Mo_2(O)_2(\mu\text{-}O)_2(\mu\text{-edta})]^{2-}$ is not available, and the structure of the similar *R*-pdta complex is referred to. It is seen from Table V that the MoW complex anion has structural characteristics very similar to those of the Mo_2–*R*-pdta and the W_2–edta complex anions. In particular, the difference in metal–metal bond distances among the three complexes amounts only to 0.017 Å. The largest difference among the main structural parameters of the three anions is seen in the distances between the metal and the terminal oxide. The distances

(46) There are some fairly large differences in bond distances and angles around M(A1) and M(B1) between the two crystallographically independent ions (see Tables III and IV). No close intermolecular contacts were found, which may cause such a difference.

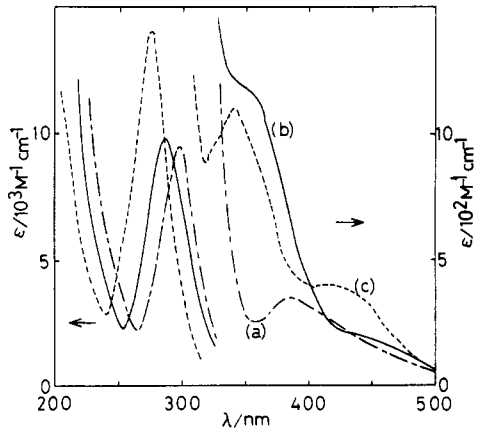

Figure 2. Electronic absorption spectra of $Na_2[M_2(O)_2(\mu\text{-}O)_2(\mu\text{-edta})]$ (M = Mo, W) in aqueous solutions: (a) $M_2 = Mo_2$; (b) M_2 = MoW; (c) $M_2 = W_2$.

are 1.68 (2)[26] and 1.74 (1) Å[31] for the Mo_2–*R*-pdta and W_2–edta complexes, respectively. The corresponding distance for the MoW complex (1.71 (2) Å) coincides with the average of the corresponding distances of the Mo_2–*R*-pdta and W_2–edta complexes. It is not possible, however, to say from the present analysis whether the two distances in the MoW complex differ by as much as 0.06 Å (difference between the two homonuclear metal complexes).

$[Mo_2(O)_2(\mu\text{-}O)_2(\mu\text{-}R\text{-pdta})]^{2-}$ has an asymmetrically distorted structure with a distorted λ-gauche conformation of the N–C–(CH_3)–C–N part.[26] Accordingly, the two distorted octahedra are twisted (torsion angle of the two Mo=O bonds (O_t–Mo–Mo–O_t) 5.4 (8)°)[26] along the metal–metal axis to give an asymmetric "Δ" configuration. The N–C–C–N part of the present mixed-metal complex also has a distorted gauche structure. Thus, each complex ion in the crystal is asymmetrically distorted along the metal–metal axis (O_t–Mo–W–O_t = 1.6 (2)°) as observed for $[Mo_2(O)_2(\mu\text{-}O)_2(\mu\text{-}R\text{-pdta})]^{2-}$. The Δ and Λ structures are paired in a unit cell. The cesium salt of the $(\mu\text{-S})_2$ complex $[Mo_2(O)_2(\mu\text{-S})_2(\mu\text{-edta})]^{2-}$ also has a distorted gauche N–C–C–N conformation.[47,48]

Electronic Absorption Spectra. Figure 2 compares the absorption spectrum of $[MoW(O)_2(\mu\text{-}O)_2(\mu\text{-edta})]^{2-}$ with those of $[Mo_2(O)_2(\mu\text{-}O)_2(\mu\text{-edta})]^{2-}$[35] and $[W_2(O)_2(\mu\text{-}O)_2(\mu\text{-edta})]^{2-}$.[31a,38] It is clear that the spectrum of the MoW complex is not the sum of those of the Mo_2 and W_2 complexes. A characteristic common feature for the three complexes is the existence of strong absorption peaks in the UV region: Mo_2 at 298 nm (ϵ = 8980 M^{-1} cm^{-1}), MoW at 288 nm (8200), and W_2 at 276 nm (14000). The peak shows a blue shift as Mo is replaced by W. The W_2 complex has a peak at 342 nm (1100) and a shoulder at ca. 422 nm (350), while the Mo_2 complex shows one peak at 388 nm (340). From a comparison of the signs of the circular dichroism maxima for the *R*-pdta complexes of Mo_2 and W_2, we concluded that the peak at 342 nm of the W_2 complex should correspond to the peak at 388 nm of the Mo_2 complex.[49,50] The distinctive shoulder at 350 nm (980) of the MoW complex probably corresponds to these transitions. There is, once again, a blue shift as Mo is replaced by W. The distinctive shoulder of the MoW complex at ca. 450 nm (140) seems to correspond to the shoulder at 422 nm of the W_2 complex. The corresponding transition of the Mo_2 complex is seen in the circular dichroism spectrum of the *R*-pdta complex at ca. 480 nm.[49]

^{1}H and ^{13}C NMR Spectra. Figure 3 shows the ^{1}H NMR spectrum at 80 °C of the MoW complex together with those of the Mo_2 and W_2 complexes. The spectrum at room temperature shows several rather broad signals in the 2.5–4 ppm region. The line broadening stems from the inversion motion of the pseudo-

(47) Spivack, B.; Dori, Z. *J. Chem. Soc., Dalton Trans.* **1973**, 1173–1177.
(48) $[W_2(O)_2(\mu\text{-}O)_2(edta)]^{2-}$ was reported to have a planar N–C–C–N structure.[31b] This may be a result of the accuracy of the analysis.
(49) Suzuki, K. Z.; Sasaki, Y.; Ooi, S.; Saito, K. *Bull. Chem. Soc. Jpn.* **1980**, *53*, 1288–1298.
(50) Ikari, S.; Sasaki, Y.; Segawa, M.; Ito, T. Unpublished results.

Table V. Average Bond Distances and Angles for $[M_2(O)_2(\mu\text{-}O)_2(\mu\text{-edta})]^{2-}$ and Related Compounds

Bond Distances (Å)

compd	M–M	M–O_t[a]	M–O_b[b]	M–O_l[c]	M–N
$Na_2[Mo_2O_4(R\text{-pdta})]\cdot 3H_2O$[d]	2.533 (2)	1.68 (2)	1.930 (5)	2.116 (7)	2.47 (2)
$Na_2[MoWO_4(edta)]\cdot 4.5H_2O$	2.55 (1)	1.71 (2)	1.94 (1)	2.09 (1)	2.40 (2)
$Ba[W_2O_4(edta)]\cdot 3H_2O$[e]	2.547 (7)	1.74 (1)	1.93 (2)	2.08 (2)	2.475 (3)

Bond Angles (deg)

compd	O_b–M–O_t	O_b–M–O_b	M–O_b–M	O_t–M–O_l	O_t–M–N
$Na_2[Mo_2O_4(R\text{-pdta})]\cdot 3H_2O$[d]	108.6 (15)	93.0 (2)	82.2 (2)	90.5 (13)	159.0 (22)
$Na_2[MoWO_4(edta)]\cdot 4.5H_2O$	109.0 (9)	92.1 (5)	82.4 (9)	92.0 (10)	158.3 (10)
$Ba[W_2O_4(edta)]\cdot 3H_2O$[e]	110.8	91.5	83.2	89.3	

[a] Terminal oxygen. [b] Bridging oxygen. [c] Coordinated oxygen of $edta^{4-}$. [d] Reference 26. [e] Reference 31.

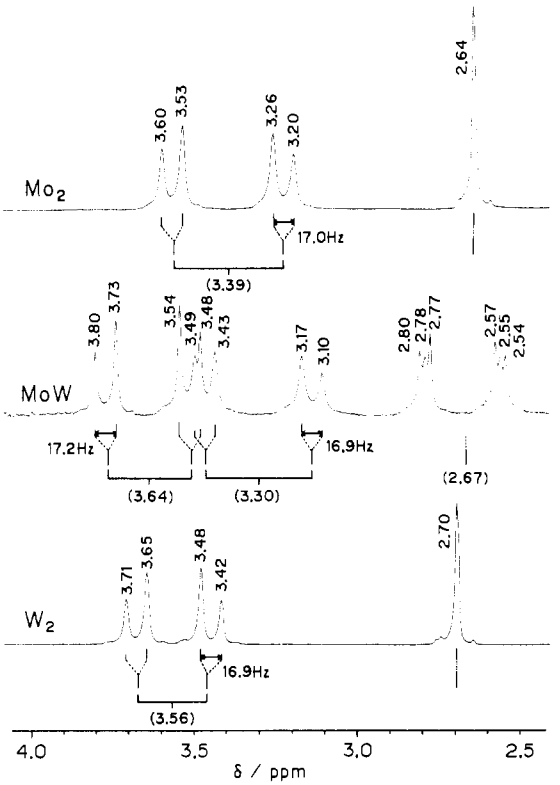

Figure 3. ^1H NMR spectra (270 MHz) of $Na_2[M_2(O)_2(\mu\text{-}O)_2(\mu\text{-edta})]$ (M_2 = Mo_2, MoW, W_2) in D_2O at 80 °C (δ = 0 for TSP) and analysis of spectral patterns (TSP = $(CH_3)_3Si(CD_2)_2COO^-Na^+$). ↔ symbols indicate coupling constants ($^2J_{H\text{-}H}$).

gauche conformation of the N–C–C–N part, which has been observed for the Mo_2[36] and W_2[51] complexes.[52] The inversion becomes sufficiently rapid at 80 °C to enable unambiguous assignment of the signals. The spectra can be regarded as rapid exchange patterns; i.e., the two acetate arms at each metal ion are equivalent on the NMR time scale. The NMR spectrum of the MoW complex is analyzed in Figure 3, and the signals are assigned with the aid of the ^1H NMR spectra of the Mo_2 and the W_2 complexes. The MoW complex shows two AB patterns centered at 3.30 and 3.64 ppm. From a comparison of the centers of gravity of AB patterns ($(\nu_A + \nu_B)/2$) and the separation of peaks ($\nu_A - \nu_B$) with those of the two homonuclear metal complexes, the signals centered at 3.30 and 3.64 ppm are assigned to acetate groups on the molybdenum and tungsten sides, respectively. The A_2B_2 pattern centered at 2.67 ppm is assigned to ethylene protons, which are nonequivalent due to the mixed-metal structure. Corresponding signals are singlets in the two homonuclear metal complexes.

(51) Sasaki, Y.; Ikari, S.; Ito, T. Unpublished results.
(52) Rate constants for the inversion have been estimated from the analysis of the ^{13}C NMR spectra as (1.01 ± 0.02) × 10^3[36] and (5.9 ± 0.1) × 10^2 s^{-1}[51] for the Mo_2 and W_2 complexes, respectively, at 25 °C.

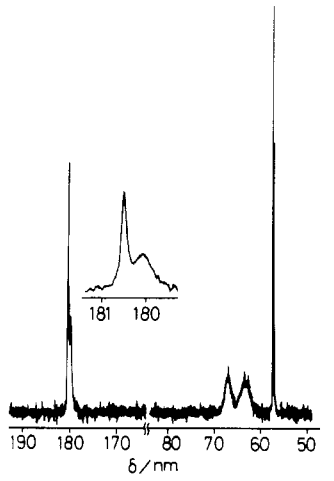

Figure 4. ^{13}C NMR spectrum of $Na_2[M_2(O)_2(\mu\text{-}O)_2(\mu\text{-edta})]$ in D_2O (δ = 0 for DSS).

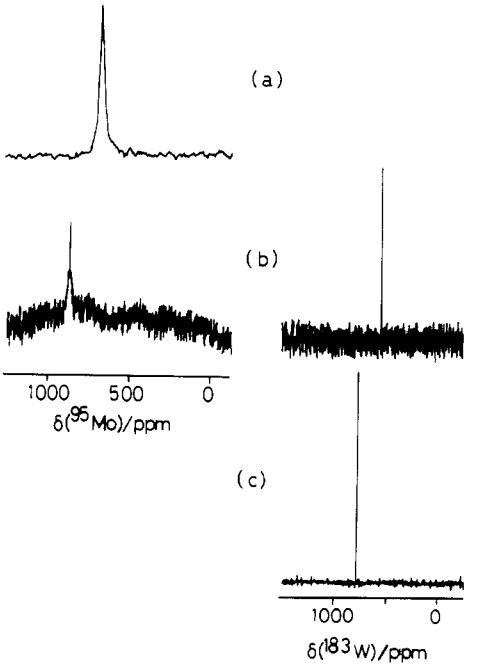

Figure 5. ^{95}Mo and ^{183}W NMR spectra of $Na_2[M_2(O)_2(\mu\text{-}O)_2(\mu\text{-edta})]$ in D_2O (relative to 1.0 M Na_2MoO_4 and 1.0 M Na_2WO_4 in D_2O for ^{95}Mo and ^{183}W, respectively): (a) M_2 = Mo_2; (b) M_2 = MoW; (c) M_2 = W_2.

The ^{13}C NMR spectrum is shown in Figure 4. The signals of ethylene, acetate methylene, and carbonyl carbons split into two in the MoW complex: 56.38 and 57.34, 66.9 and poorly resolved signals at 62.5 and 63.5,[53] and 180.12 and 180.54 ppm,

(53) Acetate methylene carbon peaks seem to split further but cannot be seen unambiguously due to broadening.

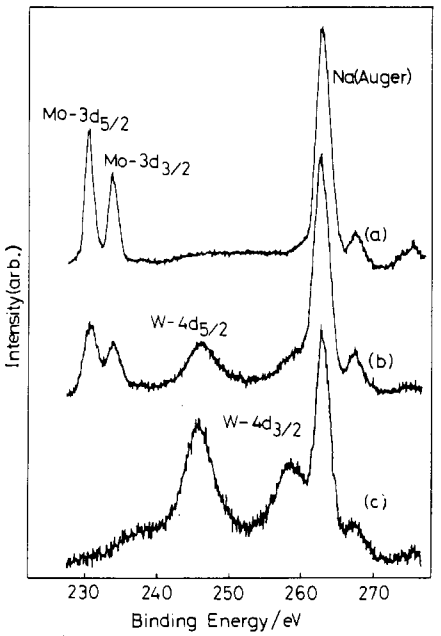

Figure 6. X-ray photoelectron spectra of $Na_2[M_2(O)_2(\mu\text{-}O)_2(\mu\text{-edta})]$ in the Mo 3d and W 4d regions (binding energies are calibrated for the C 1s (methylene part of $edta^{4-}$) peak at 284.6 eV): (a) $M_2 = Mo_2$; (b) $M_2 = MoW$; (c) $M_2 = W_2$.

Table VI. Core Electron Binding Energies[a] (eV) for $Na_2[M_2(O)_2(\mu\text{-}O)_2(\mu\text{-edta})]$ ($M_2 = Mo_2$, MoW, W_2)

M_2	Mo $3d_{3/2}$	Mo $3d_{5/2}$	W $4d_{3/2}$	W $4d_{5/2}$	W $4f_{5/2}$	W $4f_{7/2}$
Mo_2	234.7	231.5				
MoW	234.2	231.1	259.0	246.4	36.7	34.6
W_2			258.7	246.0	36.0	33.9

[a] Binding energies are calibrated for the C 1s peak (methylene part of $edta^{4-}$) at 284.6 eV.

respectively, relative to DSS at $\delta = 0$ ppm in D_2O. Further assignments of the splitting components are difficult since the corresponding chemical shifts of the two homonuclear complexes are very close to one another.[54] The shape of each signal should depend on the relative rate of conversion and the separation of the respective components.[55]

^{95}Mo and ^{183}W NMR Spectra. The spectra are shown in Figure 5. The ^{95}Mo chemical shift of the MoW complex appears at 877 ppm, which is at appreciably lower magnetic field than that (612 ppm)[4,56] of the Mo_2 complex. The ^{183}W chemical shift of the MoW complex is at 549 ppm, which is found at higher field than that (793 ppm)[4] of the W_2 complex. Thus, the direction of the shift upon mixing two metal ions is in opposite directions for the ^{95}Mo and ^{183}W chemical shifts.

X-ray Photoelectron Spectra. X-ray photoelectron spectra of the three edta complexes are shown in Figure 6, and the binding energies of Mo $3d_{5/2}$ and $3d_{3/2}$, W $4f_{7/2}$ and $4f_{5/2}$, and W $4d_{5/2}$ and $4d_{3/2}$ are summarized in Table VI. Binding energies for molybdenum are clearly lower for the mixed-metal complex than for the dimolybdenum complex, while those for tungsten are higher for the MoW complex than for the W_2 complex.

Redox Properties. Redox properties of the new mixed-metal complex were briefly studied by cyclic voltammetry. In aqueous solution at pH = 7.5 (0.2 M phosphate buffer), one irreversible oxidation wave was observed at +0.56 V vs SCE. There was no reduction wave up to −1.5 V. Potentials of both the reduction and the oxidation waves depend on pH in the case of the Mo_2 complex.[57] Thus, the potentials of the three complexes should be compared under identical solution conditions. Under these conditions, the Mo_2 and the W_2 complexes showed irreversible oxidation waves at +0.98 and +0.43 V, respectively. An irreversible reduction wave was observed at −1.34 V for the Mo_2 complex.

Discussion

Preparation and Characterization of the New Complex. The mixed-metal complex, as well as the W_2 complex, was obtained in much lower yield than the Mo_2 complex. This is probably due to the instability of the W^V monomeric ion toward oxidation compared to the Mo^V monomeric ion. The mixed-metal complex appears to be stable in neutral solution, as it does not seem to decompose during the process of the month-long ion-exchange separation procedure.

The absorption spectra, cyclic voltammetry, and various NMR spectra indicate that the complex is not a mixture of the two homonuclear metal complexes. The 1:1 ratio of Mo and W atoms is clarified by the peak intensity ratio of the XPS spectra.

The molecular structure of the new mixed-metal complex is very similar to those of the Mo_2 and W_2 complexes. This is expected since the structures of the two homonuclear metal complexes are very similar to each other. The N–C–C–N portion has a distorted gauche conformation in the solid state. The ^{1}H and ^{13}C NMR spectra indicate that rapid interconversion of the gauche conformation takes place in aqueous solution, the rate of which is probably similar to those of the Mo_2 and the W_2 complexes.[52] The analogous rates of the interconversion are related to the very similar structures and steric factors of the three complexes, and it is apparent that the different combinations of Mo and W atoms are not important. Due to the structural similarity, various properties of the MoW complex may be discussed in direct comparison with the corresponding properties of the homonuclear metal analogues.

Electronic Structure. From the data in Table VI, it is concluded that the Mo and W atoms in the MoW complex have somewhat lower and higher oxidation states, respectively, than those of the Mo_2 and W_2 complexes.[3] The metal NMR chemical shifts also point to the same conclusion for the following reason. It has been shown experimentally that the ^{95}Mo and ^{183}W chemical shifts of metal–metal-bonded di- and polymetallic complexes tend to appear at lower magnetic fields as the formal oxidation state of the complexes becomes lower.[4,58] If this trend is applicable to the present mixed-metal system, then the ^{95}Mo and ^{183}W chemical shift data indicate that molybdenum and tungsten atoms in the mixed-metal dinuclear complex have somewhat lower and higher oxidation states, respectively, than those in their homonuclear metal analogues. The results indicate that the negative charge shift from W to Mo takes place along the Mo–W bond in the MoW complex. A similar charge shift has been demonstrated previously for the trinuclear complexes with quadrivalent metal ions $[M_3(\mu_3\text{-}O)_2(\mu\text{-}CH_3COO)_6(H_2O)_3]Br_2$ ($M_3 = Mo_2W$, MoW_2) on the basis of the XPS[3] and metal NMR spectra.[4] The extent of the shifts in the metal NMR signals and also in the XPS binding energies between homonuclear and heteronuclear metal clusters may be taken as a measure of the amount of the charge shift, but the experimental data do not show an appreciable difference between the dinuclear and the trinuclear systems. The metal–metal bond distance is shorter for the dimeric system (2.55 Å) as compared with that in the trinuclear one (2.75 Å).[1] Also, in the trimeric system, one metal ion has two adjacent metal ions to share the possible charge shift. It is difficult to discuss how these factors as well as the formal oxidation number affect the

(54) The Mo_2 complex shows ^{13}C NMR signals (ppm) at 56.85 (ethylene), 63.2 and 66.7 (acetate), and 180.16 (C=O) relative to DSS at $\delta = 0$ ppm in D_2O. Corresponding signals of the W_2 complex appear at 56.79, 63.5 and 66.8, and 180.45 ppm, respectively.

(55) Apparently different coalescence behavior of the two types of acetate carbons does not necessarily mean different rates of interconversion at two different metal sites but should reflect different peak separations to coalesce. The inversion processes at the two metal sites are parts of one molecular motion and must take place simultaneously.

(56) The chemical shift of 609 ppm is also reported (Gheller, S. F.; Hambley, T. W.; Brownlee, R. T. C.; O'Connor, M. J.; Snow, M. R.; Wedd, A. G. *J. Am. Chem. Soc.* **1983**, *105*, 1527–1532).

(57) Ott, V. R.; Schultz, F. A. *J. Electroanal. Chem. Interfacial Electrochem.* **1975**, *59*, 47–60.

(58) Minelli, M.; Enemark, J. H.; Brownlee, R. T. C.; O'Connor, M. J.; Wedd, A. G. *Coord. Chem. Rev.* **1985**, *68*, 169–278.

extent of the charge density shift, since an observable difference is not seen between the two systems.

Charge density shifts are often assumed for other mixed Mo–W complexes in order to explain some of their abnormal properties.[11,17,19,23] A typical example is observed for dinuclear complexes with quadruple metal–metal bonds.[19] The ^{31}P NMR chemical shifts for the coordinated phosphines, for example, only show very small differences between the two homonuclear metal complexes $Mo_2(PR_3)_4Cl_4$ and $W_2(PR_3)_4Cl_4$. The difference, however, is remarkably large between the two kinds of ^{31}P chemical shifts in the mixed-metal complex. Such a remarkable change in the chemical shift is not observed for the ^1H and ^{13}C NMR spectra of our system. This is probably related to the distance of the ^1H and ^{13}C nuclei from the metal centers and also to the possibly small degree of the charge density shift in the present complexes.

The electronic structure of $[Mo_2(O)_2(\mu\text{-}O)_2(R\text{-cys})_2]^{2-}$ (*R*-cys = (*R*)-cysteinate(2-) ion) has been calculated by the all-valence-electron SCF MO method, and the absorption peaks in the region >250 nm have been claimed to be due to the transitions from the orbital with essentially Mo–Mo σ-bonding character to higher Mo–Mo bonding and antibonding orbitals.[59] Such a result is virtually unaffected by the difference in chelate ligands coordinated to the dimeric unit. Since the correspondence of the absorption peaks of the three Mo_2, MoW, and W_2 complexes is reasonably good, the absorption bands at >250 nm of the MoW and W_2 complexes should also be due to the transitions involving the metal–metal molecular orbitals. Thus, the electronic interaction between the two different metal ions, Mo and W, should not be significantly different in nature from those of the two homonuclear complexes. The oxidation potential of the MoW complex is between those of the two homonuclear complexes. An electron should, therefore, be removed from the Mo–W σ-bonding orbital rather than from an orbital localized on one of the metal centers.

Acknowledgment. The XPS spectra were obtained under the joint research program with the Institute for Molecular Science (1986-1987). We thank Dr. Y. Nakamura (Tokyo Institute of Technology) for ^{95}Mo and ^{183}W NMR measurements and Dr. M. Ebihara and T. Yamaguchi for the crystal structure determination.

Supplementary Material Available: Figure S1, showing a stereoscopic view of the crystal structure of $Na_2[MoW(O)_2(\mu\text{-}O)_2(edta)]\cdot 4.5H_2O$, and Tables SI, SII, SIV, and SV, listing details of the reflection data collection, anisotropic thermal parameters, bond distances, and bond angles (8 pages); Table SIII, listing calculated and observed structure factors (6 pages). Ordering information is given on any current masthead page.

(59) Brown, D. H.; Perkins, P. G.; Stewart, J. J. *J. Chem. Soc., Dalton Trans.* **1972**, 1105-1108.

Contribution from the Department of Chemistry, University of Houston, Houston, Texas 77204-5641

Synthesis, Molecular Structure, and Electrochemical Properties of Two Geometric Isomers of Tetrakis(μ-2-anilinopyridinato)dirhodium Complexes

J. L. Bear,* C.-L. Yao, L.-M. Liu, F. J. Capdevielle, J. D. Korp, T. A. Albright, S.-K. Kang, and K. M. Kadish*

Received August 31, 1988

Two geometric isomers of the tetrakis(μ-2-anilinopyridinato)dirhodium unit, $[Rh_2(ap)_4]^{n+}$ (n = 0, 1), were synthesized by using different preparative procedures. Crystal and molecular structures were determined by single-crystal X-ray diffraction and show one complex, $Rh_2(ap)_4(NCC_6H_5)$ (**1b**), to have two pyridyl and two anilino nitrogens bound to each rhodium atom trans to their own kind and to have one axially bound benzonitrile. The second complex, $Rh_2(ap)_4Cl$ (**2a**), has four pyridyl nitrogens and one chloride ion bound to one rhodium atom and has four anilino nitrogens bound to the other rhodium atom. Compound **1b**, $C_{51}H_{41}N_9Rh_2$, crystallizes in the orthorhombic space group *Pbca* with eight formula weights in a unit cell of dimensions a = 21.002 (7) Å, b = 17.317 (6) Å, and c = 26.028 (8) Å and refined to R = 0.063. Compound **2a**, $C_{44}H_{36}N_8ClRh_2$, crystallizes in the monoclinic space group $I2/c$ with four formula weights in a unit cell having dimensions a = 20.321 (5) Å, b = 9.594 (2) Å, c = 21.273 (4) Å, and β = 111.35 (2)°, with final R = 0.031. Compound **1** (**1b** without axial benzonitrile) undergoes two reversible one-electron oxidations in CH_2Cl_2, 0.1 M TBAP, at 0.08 and 0.82 V vs SCE. Complex **2a** is reversibly reduced by one electron at -0.38 V and reversibly oxidized by one electron at 0.52 V in CH_2Cl_2. Electrochemical studies show that compound **1a** (singly oxidized **1**) forms bisadducts of Cl^-, CN^-, or CH_3CN in CH_2Cl_2 solutions containing high concentrations of these ligands whereas **2a** exists only as a monoadduct. The ESR spectra of **1a** (rhombic signal with g_3 split into a 1:2:1 triplet) and **2a** (axial signal with $g_\parallel$ split into a doublet) are consistent with the singly occupied molecular orbital (SOMO) being equally distributed on both Rh atoms in the former complex and being localized on one rhodium atom in the latter. Extended Hückel calculations were carried out on $[Rh_2(O_2CH)_4]^+$, $[Rh_2((NH)_2CH)_4]^+$, and $[Rh_2((NH)_2CH)_4(L)]^+$, and the mechanisms for localization of the odd electron on **2a** are discussed.

Introduction

The synthesis and spectroelectrochemical characterization of a dinuclear rhodium complex containing four 2-anilinopyridinate ligands (ap) were first reported by Tocher and Tocher.[1] The orientation of the bridging 2-anilinopyridinate ions was not determined for the reported complex, and it was not known which of the four possible geometric isomers was synthesized. Our laboratory was successful in obtaining two geometric forms of the tetrabridged complex, and we reported preliminary results on the structure, electrochemistry, and ESR properties of these species.[2] One of the two isomers has a (2,2-trans) donor atom arrangement, which consists of two pyridyl (N_p) and two anilino (N_a) nitrogens on each rhodium atom bound trans to their own kind (compound **1**). The other isomer (compound **2**) has a (4,0) arrangement with four pyridyl nitrogens bound to one rhodium atom and four anilino nitrogens bound to the other rhodium atom.

The different bonding arrangement of the pyridyl and anilino nitrogens has a significant effect on the UV–vis and ESR spectra of the two isomeric forms. The singly oxidized form of compound **1** (called compound **1a**) has a rhombic ESR signal with g_3 split into a 1:2:1 triplet, whereas the radical cation of **2** (called compound **2a**) shows an axial signal with $g_\parallel$ split into a doublet. These results are consistent with the spin density of the odd electron being distributed equally on both rhodium ions in the former complex

(1) Tocher, D. A.; Tocher, J. L. *Inorg. Chim. Acta* **1985**, *104*, L15.
(2) Bear, J. L.; Liu, L.-M.; Kadish, K. M. *Inorg. Chem.* **1987**, *26*, 2927.

0020-1669/89/1328-1254$01.50/0